JOURNAL OF MATERIALS SCIENCE 23 (1988) 1995–2013

Ultrasonic relaxation spectra in CoO–Co_2O_3–P_2O_5 glasses in the temperature range 6 to 300 K

B. BRIDGE, A. A. HIGAZY*
Physics Department, Brunel University, Kingston Lane, Uxbridge, Middlesex UB8 3PH, UK

Formulae attributing acoustic relaxation in glasses to two-well systems with a distribution of barrier heights and asymmetries are related to the phenomenological theory of a standard linear solid. Acoustic wave loss measurements at frequencies ranging from 15 to 135 MHz and temperatures ranging from 6 to 300 K have been used to compute relaxation spectra for the CoO–P_2O_5 glass system. For each glass two alternative sets of spectra have been deduced on the contrary assumptions that the range of asymmetries is very broad, or very narrow. From the quality of the fit of theory with experiment, it is concluded that the former description is more likely to be applicable to the glasses. From the systematic nature of the composition dependence of several of the acoustic parameters it is concluded that a broad relaxation spectrum is to be associated with P_2O_5 structural groupings, whilst a much narrower spectrum obtains for metaphosphate and pyrophosphate groupings. The spectral analysis also showed that in all the glasses there is evidence of the existence of two-level systems which produce a pronounced upturn in the acoustic relaxation loss at temperatures below 40 K. Since accurate absolute attenuation data were required for the purpose of evaluating alternative relaxation spectra, attenuation measurement errors are analysed in some detail. As the present work is part of a long-term programme of study on the composition dependence of low-temperature ultrasonic properties of glasses, the methods by which slow sweeps of sample temperature from 4 to 300 K are achieved with maximum economy of helium consumption are discussed in some detail.

1. Introduction

The existence of peaks in the temperature dependence of acoustic wave absorption occurring in the range of a few degrees Kelvin to 300 K, is widespread, possibly universal, in inorganic glass systems, and have been the subject of several recent review articles [1–4]. On account of the characteristic frequency dependence of the loss peak temperature it has been generally assumed that the loss is formally attributable to the thermal motion of particles or excitations moving in two-well systems with dimensions of an atomic order of magnitude. Attempts to quantify this distribution have not, so far, been very successful. On any reasonable set of assumptions the number of two-well systems per unit volume required to explain the magnitude of the loss peaks is typically of the order of 1% of the number of atoms per unit volume. This has caused speculation that in a given material the two-well systems derive not from the network structure as a whole, as suggested by Bridge and Patel [5], but from minor structural features such as impurities, network holes or OH groups. We suggest that the best way to resolve this issue one way or the other is to study the loss peaks as a function of gradual changes in a glass structure. A systematic variation in the parameters of the two-well description with composition, within a single binary glass system, could be dismissed as a coincidence. However, if systematic variations in these parameters with composition occur in a number of binary glass systems, the overwhelming probability is that the two-well parameters are properties of a glass network as a whole. For this reason a study of ultrasonic relaxation throughout the entire composition range of a number of binary phosphate glass systems was commenced by Bridge and co-workers. The present data on CoO–P_2O_5 glasses follows on from previously published work on the MoO_3–P_2O_5 system [5–9]. Prior to this comprehensive programme, the quite substantial amount of previous work on other glass systems (hardly any data existed on phosphate glasses) was carried out in a rather *ad hoc* manner, only the effect of gross composition changes being examined, in effect.

In the present paper out interest is focused on the possible distribution functions (relaxation spectra) for two-well parameters that can be fitted to the shape of

Present address: Monafia University, Sheebeen el Koume, Egypt.

0022–2461/88 $03.00 + .12

the observed loss peaks. In spite of a wealth of loss peak data, relatively little attention has been given to the systematic study of such experimentally determined distribution functions in the past literature, although the use of standard functions has been examined in some detail [10, 11]. Yet, although the procedure is laborious, the advantage of deriving a relaxation spectrum is that whilst containing implicitly all the information about the loss behaviour, it depends only on the material and not on the temperature or propagation frequency. Thus it comprises a useful, concise method of presenting acoustic data for discussions of composition dependence, even if the physical significance of the two-well formalism is open to doubt [12].

2. General considerations

There is an inelegant proliferation of formulae in existing literature on acoustic relaxation in glasses. In the present discussion we bring together many of the relevant relationships and relate them to general phenomenological theory. Consider two springs for which the ratios of stress, σ, to strain, ε, are ΔM and $M - \Delta M$, respectively and a viscous dashpot for which the ratio of applied stress to the rate of change of strain is $\Delta M\tau$. If the dashpot and first spring are connected in series across the second spring which is clamped at one end, the stress–strain relationship for the spring is readily shown to be

$$\sigma + \tau\dot{\sigma} = (M - \Delta M)\varepsilon + M\tau\dot{\varepsilon} \qquad (1)$$

If M, ΔM and τ are constants, Equation 1 defines the stress–strain relationship at any point in a so-called "standard linear solid". Substituting this relation into the general wave equation for one-dimensional motion $\partial^2\sigma/\partial x^2 = \varrho\ddot{\varepsilon}$, where ϱ is the density, the internal friction Q^{-1} and dispersion in phase velocity, for plane waves of angular frequency ω in the limit $\Delta M \ll M$ (low dispersion) are given by

$$Q^{-1} = \frac{2\alpha c}{\omega} = \frac{\Delta M}{M}\left(\frac{\omega\tau}{1 + \omega^2\tau^2}\right) \qquad (2)$$

$$\frac{\Delta c}{c} = \frac{-1}{2}\frac{\Delta M}{M}\left(\frac{1}{1 + \omega^2\tau^2}\right) \qquad (3)$$

where

$$c = (M/\varrho)^{1/2} \qquad (4)$$

Here α is the wave absorption in nepers per unit length, Δc is the difference between the phase velocity at frequency ω and the phase velocity c for $\omega \to \infty$. It is also convenient to note that M is the elastic modulus $(\partial\sigma/\partial\varepsilon)$ governing the wave propagation at $\omega \to \infty$ (the unrelaxed modulus), $M - \Delta M$ is the elastic modulus at $\omega > 0$ (the relaxed modulus), τ is the stress relaxation time (time taken for σ to reduce by a factor e^{-1}) at constant strain, and $\Delta M/M$ (the fractional difference between the unrelaxed and relaxed modulus) is frequently known as the relaxation strength.

When there is a distribution of relaxation processes of different relaxation times and corresponding relaxation strengths, the resultant internal friction and phase velocity shift are obtained straightforwardly by the principle of superposition, i.e.

$$Q^{-1} = \int_0^\infty \frac{\delta(\Delta M/M)\,\omega\tau}{1 + \omega^2\tau^2} \qquad (5)$$

$$\frac{\Delta c}{c} = \frac{-1}{2}\int_0^\infty \frac{\delta(\Delta M/M)}{1 + \omega^2\tau^2} \qquad (6)$$

where $\delta(\Delta M/M)$ is the relaxation strength of the relaxing systems with relaxation times in the range τ to $\tau + d\tau$, i.e. the contribution to the fractional difference between the unrelaxed and relaxed moduli of the solid, caused by those systems. Thus the total fractional difference between the unrelaxed and relaxed moduli caused by all systems with relaxation times in the range 0 to ∞ is given by

$$\frac{\Delta M}{M} = \int_0^\infty \delta(\Delta M/M) \qquad (7)$$

Many loss mechanisms in a macroscopically homogeneous solid can produce an internal friction and phase velocity dispersion of the form of Equations 2 and 3, at least in a first approximation. One of these is the particle in a two-well potential, of dimensions small compared with the acoustic wavelength so that each particle always moves in a strain field of constant phase. For a spatially uniform distribution of n, identical wells per unit volume of central barrier height V and asymmetry (separation of the well minima) Λ, classical thermodynamical arguments [13] (see Appendix) show that the loss is given by Equation 2 with

$$\frac{\Delta M}{M} = -\frac{nD^2}{\varrho c^2}\frac{d}{d\Lambda}\left(\frac{1}{1 + \exp(\Lambda/kT)}\right) \qquad (8)$$

and

$$\tau = 2\tau_0 \exp\left(\frac{V}{kT}\right)\left[1 + \exp\left(\frac{\Lambda}{kT}\right)\right]^{-1} \exp\left(\frac{\Lambda}{2kT}\right) \qquad (9)$$

where V is measured from the mean value of the two minima, k is Boltzmann's constant, T is the absolute temperature, $(2\tau_0)^{-1}$ is the classical vibration frequency (attempt frequency) for the particle in either well, and $D = \partial\Delta/\partial\varepsilon$ denotes the "coupling" between the acoustic wave and the well (deformation potential).

In general there will be a distribution of D, τ_0, Λ and V values amongst a large number of two-well systems having any given orientation relative to the direction of strain. In addition, D will be orientation-dependent and in subsequent discussions an orientationally averaged value of D will be assumed. D (so averaged) and τ_0 will be functions of well geometry and it is reasonable to assume that the spread of D, τ_0, V and Λ in percentage terms will be of the same order. However, Λ and V appear in the argument of an exponential in Equations 5 and 6. At a typical loss peak temperature of 100 K, $\omega\tau$ will vary by many orders of magnitude when V varies from 0.01 to 0.1 eV. Under these conditions it is reasonable to assume constant "average" values for D and τ_0 when considering a loss due to a distribution of two-well systems. Thus for n two-well systems per unit volume, the internal friction

is given by Equation 5 with τ given by Equation 9 (taking τ_0 as a contant), and

$$\delta(\Delta M/M) = \frac{D^2}{\varrho c^2}\frac{\mathrm{d}}{\mathrm{d}\Lambda}\left(\frac{1}{1+\exp(\Lambda/kT)}\right) \times n(V)n(\Lambda)\,\mathrm{d}V\,\mathrm{d}\Lambda \quad (10)$$

where $n(V)\,\mathrm{d}V$ is the number of two-well systems with barrier height in the range V to $V + \mathrm{d}V$, i.e.

$$\int_0^\infty n(V)\,\mathrm{d}V = n \quad (11)$$

and $n(\Lambda)\,\mathrm{d}\Lambda$ is the number of two-well systems with barrier height in the range V to $V + \mathrm{d}V$ having asymmetries in the range Λ to $\Lambda + \mathrm{d}\Lambda$. Although the distribution of Λ values could run from $-\infty$ to $+\infty$ the range of integration for Λ is taken as 0 to ∞ because the averaging of D over all orientations allows for both positive and negative Λ.

It is generally accepted that a broad distribution of barrier heights is required to explain the width of internal friction peaks occurring in glasses in the range a few degrees Kelvin to 300 K. The loss given by Equation 5 with τ taken from Equation 9 becomes vanishingly small when $V \to 0$ or ∞ whilst if the $n(V)$ function is peaked around some value V_p given by the experimentally observed relation for glasses

$$\omega(\tau_0)_p \exp(V_p/kT_p) \approx 1 \quad (12)$$

where T_p is the loss peak temperature, the loss peak given by Equation 7 is much too narrow, irrespective of the form of $n(\Lambda)$. No such restrictions apply to the latter function, and we can envisage the two extreme situations described below.

2.1. A broad distribution of asymmetries such that $n(\Lambda)$ is uniform over a range $\Lambda = 0$ to $|\Lambda|_{max} > 2kT$

Writing $n(\Lambda) = n_0$, a constant, and assuming a cut-off in the integration over Λ at $\Lambda = 2kT$ on the grounds that the contributions to the integral are small for $|\Lambda| \gtrsim 2kT$, and assuming further that sech $(\Lambda/2kT) \approx 1$ for $\Lambda \lesssim 2kT$, the substitution of Equation 10 into Equation 5 yields [5, 10]

$$Q^{-1} = \int_0^\infty \frac{C(V)\omega\tau\,\mathrm{d}V}{1+\omega^2\tau^2} \quad (13)$$

where

$$\tau = \tau_0 \exp(V/kT) \quad (14)$$

and

$$C(V) = \frac{D^2 n_0 n(V)}{2\varrho c^2} \quad (15)$$

Thus $C(V)\,\mathrm{d}V$ is the relaxation strength of the two-well systems of barrier height in the range V to $V + \mathrm{d}V$, i.e. in the notation of the general phenomenological model, the standard linear solid (Equations 5 and 7), the effective contribution to $\Delta M/M$ from two-well systems having barrier height in the range V to $V + \mathrm{d}V$ is*

$$\delta(\Delta M/M)' = C(V)\,\mathrm{d}V \quad (16)$$

and

$$\frac{\Delta M}{M} = \int_0^\infty C(V)\,\mathrm{d}V \quad (17)$$

Since the relaxation strength is independent of temperature we shall, for brevity, describe this as the temperature-independent coupling (TIC) case.

2.2. Symmetric wells only or a distribution of asymmetries for which $n(\Lambda)$ is significant only for $\Lambda/kT \ll 1$

Substitution of Equation 10 into Equation 5 now produces

$$Q^{-1} = \frac{1}{kT}\int_0^\infty \frac{C(V)\,\mathrm{d}V\omega\tau}{1+\omega^2\tau^2} \quad (18)$$

where

$$\tau = \tau_0 \exp(V/kT) \quad (19)$$

and

$$C(V) = \frac{D^2}{4\varrho c^2} n(V) \quad (20)$$

Thus $(1/kT)C(V)\,\mathrm{d}V$ is the relaxation strength of the two-well systems having barrier heights between V and $V + \mathrm{d}V$, i.e.

$$\delta(\Delta M/M) = \frac{1}{kT}C(V)\,\mathrm{d}V \quad (21)$$

and

$$\frac{\Delta M}{M} = \frac{1}{kT}\int_0^\infty C(V)\,\mathrm{d}V \quad (22)$$

Since the relaxation strengths are proportional to reciprocal absolute temperature, we shall describe this as the temperature-dependent coupling (TDC) case.

On grounds of simplicity it is usually more convenient to use the $C(V)$ notation in preference to $\delta(\Delta M/M)$, and we shall employ the former in most of this paper, as have other workers. However, the use of the latter notation is invaluable in unmasking some interesting basic physics, i.e. the relationship between the integral over the "relaxation spectrum" and the extremal elastic moduli of a linear solid.

For the purposes of numerical fitting of Equations 13 and 17 to experimental data it is necessary to use summation functions. Thus for the TIC case

$$Q^{-1} = \sum_i \frac{C_i\omega\tau_i}{1+\omega^2\tau_i} \quad (23)$$

with

$$\tau_i = \tau_0 \exp(V_i/kT) \quad (24)$$

and

$$C_i = C(V)\delta V = \frac{D^2 n_0}{2\varrho c^2} n(V)\delta V \quad (25)$$

where

$$\delta V = V_i - V_{i-1} \quad (26)$$

the energy interval used in the summation, and now

$$\frac{\Delta M}{M} = \sum C_i \quad (27)$$

*The prime distinguishes the left-hand side of Equation 16 from the left-hand side of Equation 10, where the integration over Λ has not been carried out.

For the TDC case

$$Q^{-1} = \frac{1}{kT}\sum_i \frac{C_i\omega\tau_i}{1+\omega^2\tau_i} \quad (28)$$

where

$$\tau_i = \tau_0 \exp(V_i/kT) \quad (29)$$

$$C_i = C(V)\delta V = \frac{D^2}{4\varrho c^2} n(V)\delta V \quad (30)$$

δV being defined as previously, and now

$$\frac{\Delta M}{M} = \frac{1}{kT}\sum C_i \quad (31)$$

A suitable value to adopt for τ_0 for both TIC and TDC cases would be the quantity $(\tau_0)_p$ determined experimentally from Equation 12.

3. Experimental procedure

3.1. Glass sample preparation

Glasses were obtained by melting together Co_3O_4 and P_2O_5 reagents in open crucibles and full details about preparation and chemical analysis have been published elsewhere [14]. The composition of the glasses took the form $x\text{CoO} \cdot y\ \text{Co}_2\text{O}_3 \cdot (1-x-y)\ \text{P}_2\text{O}_5$, where the ratio of x to y decreased gradually to zero with increasing x. However, the degree of reduction of the initial Co_2O_4 was so high that for present purposes it is sufficient to decribe the glasses as a binary $CoO–P_2O_5$ series. The preparation of glass rods with end-faces optically polished and parallel to within 1 to 2 seconds of arc, as required for high-precision ultrasonic measurements, has been described previously [15].

From the large number of $CoO–P_2O_5$ glasses prepared, seven glasses were selected for low-temperature studies. These glass compositions were chosen so that the composition dependence of the measured properties would be adequately defined, given that composition regimes were anticipated in which these properties varied rapidly, like previously described ultrasonic properties at room temperature [15]. The number of glasses chosen was just about adequate for the above purpose: ideally a few more would have been advantageous, but this was not feasible in terms of the budget for liquid ^{4}He consumption available for the project.

3.2. Sample holder

Glass rods of 13 mm diameter and 5 mm long were employed (Fig. 1). Uncoated 1 cm dia. quartz X-cut transducers, operating at their fundamental resonant frequency (15 MHz nominal) or one of their odd harmonics, were used as a common transmitter and receiver. The transducer was coupled to a glass rod by means of Nonaq stopcock grease (Fischer Scientific Company, Fairlawn, New York State), a constant contact pressure being maintained by means of a spring-loaded contact button which also acted as one electrode. The contact pressure could be adjusted to obtain the best echo pattern by turning a knurled wheel at the bottom of the sample supporting frame; this advanced the contact button by means of a screw-thread locating in a nut in the bottom plate of the sample supporting frame, the screw axis being concentric with the sample. All glass rods were coated with a thin film of aluminium by means of vacuum evaporation, to provide the second electrode. The top of the sample supporting frame was attached by a second screw and nut arrangement to a holder supplied by Oxford Instruments Ltd (Osney Mead, Oxford, UK). The holder supported the sample near the bottom of the cryostat and carried the coaxial transducer cable and leads for two calibrated gold–chromel–copper–constantan thermocouples through coaxial seals in the cryostat lid. One thermocouple used to monitor the sample temperature was strapped to the sample supporting frame and lay within 0.5 mm of the sample circumference, whilst the reference thermocouple (in series with the first) was maintained at ~80 K by immersion in liquid nitrogen.

Figure 1 Sample holder for 4 to 300 K ultrasonic measurements.

3.3. Sample temperature control

Since, as described in our introduction, composition-dependence experiments on many glass systems were planned in the long term, it was essential to have the most economical possible method of sweeping glass sample temperatures from 4 to 300 K. The system decided on was an Oxford Instruments CF 500 continuous flow cryostat (Fig. 2). A purpose-built system for sweeping the temperature of the sample chamber from 4 to 300 K, consisting of a DTC2 temperature controller, gas flow pump, flow controller and flow meter mounted on a portable trolley, was also supplied by Oxford Instruments. The cryostat was specially designed for low ^{4}He consumption, with an integral transfer tube which fitted directly into the top of a helium storage vessel. The standard CF500 unit has an inner diameter at the "cold end" (i.e. in the sample chamber) of 20 mm. However, to permit

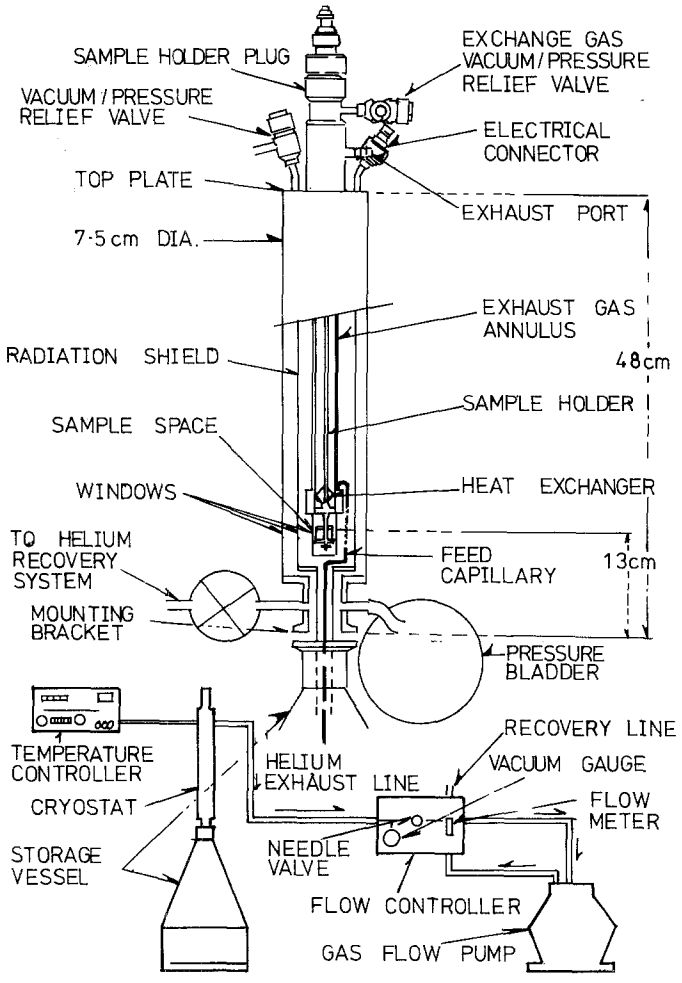

Figure 2 Schematic diagrams of the low helium consumption continuous-flow cryostat.

ultrasonic measurements on glass rods up to 15 mm diameter, in the interests of high absolute accuracy of attenuation measurements, a modified unit with sample chamber diameter increased to 25 mm was constructed. The lowest sample temperatures achieved, due presumably to the combined effects of these alterations and the size and nature of the sample, was 6 K (at no stage does liquid helium make contact with the sample in the CF500 instrument).

After obtaining the best exponential echo pattern at room temperature the specimen holder was placed into the inner tube of the cryostat. The inner tube was evacuated with a rotary pump (pressure about 1 torr), while the outer chamber of the cryostat was previously evacuated for 24 h at a pressure of 3×10^{-3} torr using a combined rotary/diffusion pump system. Next the integral transfer tube was slowly lowered into a helium storage vessel, and the gas flow control console subsequently connected (using the polythene line provided to the gas flow pump) to the cryostat and the helium recovery line. The gas flow pump was switched on to allow the helium gas to flow from the storage vessel up to the integral transfer tube. through the feed capillary and into the exchanger. The helium exhausts up through an annular space around the sample tube and passes through a second heat exchanger at the top of the cryostat. The electrical connections between the temperature controller, the heater and the temperature sensor were then completed. However, during the cool-down the temperature controller was set in the manual position with the heater off. So, within half an hour, the cryostat cooled down to about 5 K by the passage of helium gas at high flow rates (about $21\,h^{-1}$) through the cryostat.

The flow rate was then reduced to $\sim 0.21\,h^{-1}$, and then the temperature was raised to the required value by means of the electric heating coil (attached to the exchanger), which could be controlled either manually or automatically by the temperature controller. The temperature controller was set sequentially at temperatures of 5, 10, 20, 30, etc. up to 300 K, in each case a time of about seven minutes after each controller adjustment being allowed for the glass to reach a state of thermal equilibrium. (Typically after such a period of time no further changes in the ultrasonic properties being measured could be observed.)

The temperature of the specimen was monitored by two pre-calibrated gold–chromel–copper–constantan thermocouples, which were attached to the specimen and the error in sample temperature measurement is estimated to be ± 0.2 K. At the completion of an experiment the coolant flow was stopped by switching off the gas flow pump. After a few seconds the helium exhaust line can be disconnected from the cryostat and then the cryostat removed from the storage vessel. The total time of each experiment (cool-down time plus warm-up time) was about 6 h.

Usually from a 17 litre Dewar of helium (supplied by British Oxygen Co.) we managed to perform five runs from 4 to 300 K, four of which were used to measure attenuation in the same glass sample at frequencies of 15, 45, 75, 105 MHz, whilst the fifth run

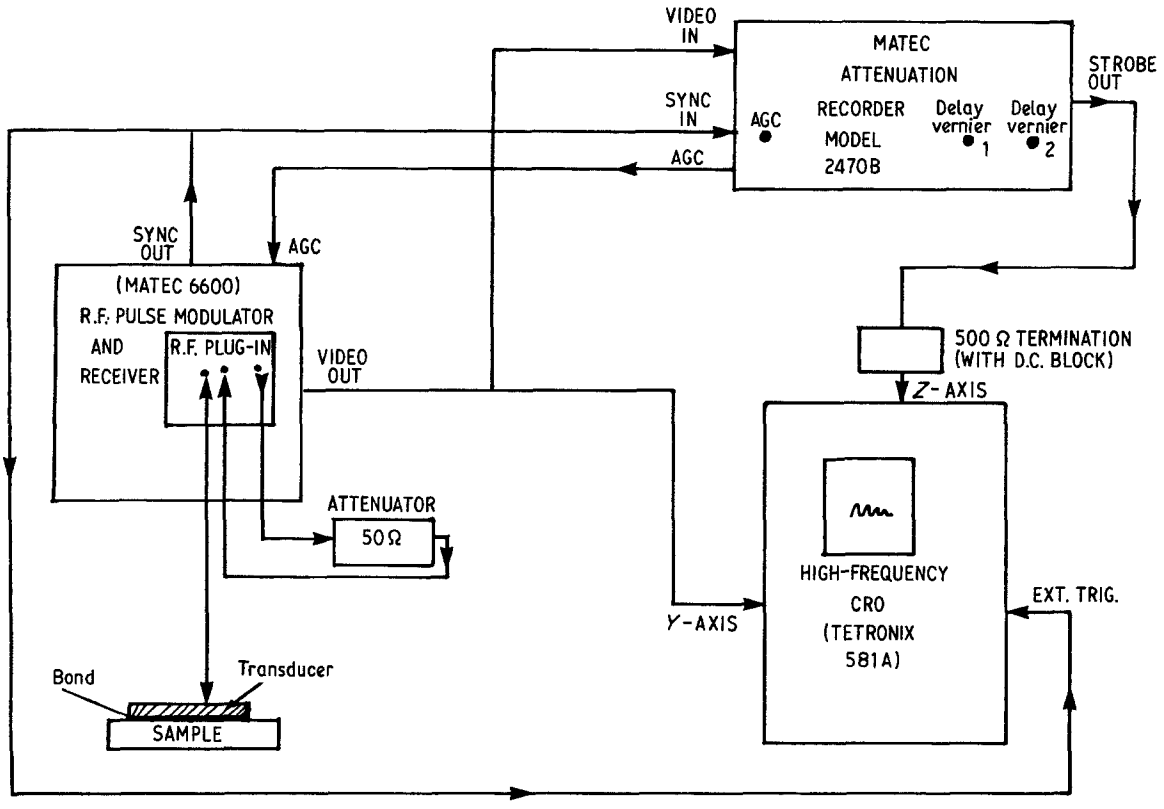

Figure 3 Block diagram of instrumentation for automatic ultrasonic wave attenuation measurements.

was employed to measure attenuation at 135 MHz (when echoes were obtainable) or the velocity at 15 MHz, in the same sample. In all, to complete this scheme of measurements in the seven selected glasses, eight Dewars of helium costing ~£2000 at current prices) were employed.

3.4. Instrumentation for ultrasonic wave attenuation measurement

Pulse echo equipment supplied by Matec Inc. (Warwick, USA) was employed for the generation, reception and processing of ultrasonic echoes (Fig. 3). This consists of a pulse modulator and receiver mainframe (Model 6600) into which could be plugged a number of r.f. oscillator units to cover a frequency range continuously variable from 1 to 700 MHz. The plug-ins available for our use were the 755V (1 to 20 MHz), 760V (10 to 90 MHz), 765V (90 to 360 MHz), and 770V (300 to 700 MHz). The typical pulse power output is 0.5 to 1 kW and the intermediate-frequency bandwidth of the superheterodyne receiver is 4 MHz centred on 30 MHz. The overall receiver gain is 110 dB and the receiver is linear for up to 8 V output, making acoustic attenuation measurements on video pulses feasible. The amplitude difference in dB between the peaks of any two video pulses of interest was measured using the Model 2970B automatic attenuation recorder. Synchronized by the 6600 mainframe, the attenuation unit provides automatic gain control (AGC) for the receiver, resulting in an echo display on a cathode-ray oscilloscope (CRO) quite exceptionally free of pulse height jitter due to variations in transmitter output or other causes. A strobe output from the recorder was used to modulate the CRO so that echoes selected by the recorder for measurement were conveniently identified by appearing bright in a dimmed-out CRO display. Using the built-in meter attenuation ranges of 1, 2, 5, 10 and 20 dB full-scale were possible and via a control providing 0 to 20 dB of variable offset, total attenuations of up to 40 dB could be measured (the maximum attenuation encountered between the selected echoes in our experiments). The maximum sensitivity, using the 1 dB full-scale setting was 0.01 dB per division. The r.f. oscillators were operated at maximum output amplitude to achieve the best pulse shape, as recommended in the Matec operating manual. The first selected echo was then arranged to be well less than 8 V by the use of 50 Ω step attenuators at the receiver input (Models 50 HT 82.5, 0 to 82.5 dB in 0.5 dB steps; 50 HT 42, d.c. to 700 MHz, 0 to 42 dB in 1 dB steps, supplied by Matec).

Procedures for minimizing the numerous sources of error in attenuation followed the practices recommended by Truell *et al.* [16] and McSkimin [17] for minimizing the "apparent" or "unwanted" attenuation which is not caused by interactions with the sample structure but by geometrical, bond and bandwidth (tuning) effects. Thus apparent attenuation was assumed to be a minimum when the observed attenuations between many successive pairs of echoes were in closest agreement, i.e. the decay envelope was closest to exponential, and at the same time this attenuation between the earliest echoes was the smallest observed. This condition does not normally occur when the first echo is a maximum but when the number of echoes observable is a maximum. Successive adjustments to the bond and the tuning controls of the Matec plug-ins prior to each low-temperature run were carried out in accordance with the above procedure.

3.5. Assessment of errors in sample attenuation measurement

Since we are relying on our attenuation measurements to decide which of two alternative relaxation spectra best fit the data, an assessment of the errors in absolute attenuation would be desirable. The known quantifiable contributions to the apparent attenuation are as follows:

(i) Due to mode conversion at the sample side-walls [17]

$$\alpha_{mc} \approx \frac{4.73c(1 - R^2)}{\omega a^2} \quad \text{dB cm}^{-1} \qquad (32)$$

where a is the tranducer radius and R is the power reflection coefficient for the incident compressional wave-mode appropriate to the angle of incidence on the sidewalls. The maximum value of the attenuation is therefore

$$(\alpha_{mc})_{max} = \frac{4.73c}{\omega a^2} \quad \text{dB cm}^{-1} \qquad (33)$$

(ii) Due to beam spreading (diffraction) caused by the finite transducer aperture, the attenuation of an echo having travelled a distance x before its return to the transducer is

$$\alpha_d(x) = \overline{|P(x)_{max}|} \qquad (34)$$

which is the pressure amplitude time averaged and spatially averaged over the transducer cross-section, measured in decibels below the same quantity for the initial pulse ($x = 0$). This attenuation is an increasing function of x but with minima superimposed at $0.73\,a^2/\lambda$, $1.05\,a^2/\lambda$ and $2.4\,a^2/\lambda$ (λ = wavelength) for the range over which it has been calculated [16] ($x = 0$ to $5\,a^2/\lambda$). However, to a first approximation

$$\alpha_d(x) = 1.8\left(\frac{x\lambda}{a^2}\right)^{1/2} \quad \text{dB} \qquad (35)$$

(iii) Due to a wedge angle θ between the propagation direction of a returned echo and the transducer, the attenuation relative to the critical (transmitted pulse) after n specimen transits is

$$\alpha_\theta(n) = 20 \log_{10}\left[\frac{2J_1(2Kan\theta)}{2Kan\theta}\right] \quad \text{dB} \qquad (36)$$

where $K = c/\omega$. For $2Kan\theta \ll 1$ the term in square brackets simplifies to $\exp[-\{(2Kan\theta)^2/8\}]$ so that

$$\alpha_\theta(n) \approx 4.343\frac{\omega^2 a^2 n^2 \theta^2}{c^2} \quad \text{dB} \qquad (37)$$

The wedge angle θ may arise either from non-parallel sample faces or from a wedge-shaped bond, but in our subsequent error calculation we shall assume that the latter contribution was negligible after using echo decay envelope inspection to adjust the bonds. As for the former contribution, θ was found optically (on a microptic measuring machine, vertical pattern, Hilger and Watts Ltd) to be within 2 to 3 seconds of arc. A velocity gradient $\partial c/\partial x$ down the sample caused by sample inhomogeneities also produces an apparent attenuation given by the above equations, with $\theta = x(\partial c/\partial x)/c$.

Using Equations 33, 35 and 37 we have calculated the apparent attenuation due to the above causes separately and combined for a typical $CoO–P_2O_5$ glass ($c \approx 4000\,\text{m sec}^{-1}$) at the extremal frequencies, assuming that θ is 2 seconds of arc ($\approx 10^{-5}$ rad). The calculated differences between the attenuations of the third and first echoes has been divided by four times the sample thickness to express the data in dB per unit length in Table I, when they are also compared with the measured peak attenuation.

When the sample temperature changes, α_{mc}, α_d and α_θ hardly change so that irrespective of the size of these quantities and whether they have been allowed for, all observed changes of "true" sample attenuation with temperature are considered to be reproducible to about $\pm 2\%$. Attenuation readings for any given glass, frequency or temperature are also considered repeatable to about $\pm 2\%$, with due care.

4. Analysis of results

In Fig. 4 the temperature dependences of the internal friction of the seven glasses are compared, at 45 MHz. In Fig. 5 plots of $\log \omega$ against T_p^{-1} are given, and the excellent correlation coefficient in a linear regression analysis (98 to 99%) suggests that the two-well formalism of acoustic relaxation is applicable. Using the 45 MHz experimental data, Equations 23, 24, 28 and 29 have been used to obtain the relaxation spectrum, i.e. dependence of C_i on V_i, for each glass, for both the TIC and TDC cases (Figs 6 and 7, respectively). The constant values of τ_0 used in Equations 24 and 29, for each glass, were taken as equal to $(\tau_0)_p$ obtained from the application of Equation 12 to the $\log\omega$ against T_p^{-1} plots. Values of $(\tau_0)_p$, one-half of the reciprocal of which might be regarded as some kind of average classical vibration frequency for the two-well excitations or particles, are given in Table I. In Fig. 8 the temperature and frequency dependence of the observed attenuation (in dB μsec^{-1}) is plotted in the ranges 6 to 300 K and 14 to 135 MHz, respectively (hollow circles). The solid lines represent the theoretical

TABLE I Comparison of theoretical attenuation due to geometrical effects (α_{mc}, α_d and α_θ) and the observed peak loss in a typical $CoO–P_2O_5$ glass, based on observation of the first and third echoes in a 5 mm thick sample with $a = 5$ mm, $c = 4000\,\text{m sec}^{-1}$ and $\theta = 2$ seconds of arc

Frequency (MHz)	α_{mc} (dB cm^{-1})	α_d (dB cm^{-1})	α_θ (dB cm^{-1})	Total apparent attenuation (dB cm^{-1})	Observed peak loss (dB cm^{-1})	Total apparent attenuation as a fraction of the peak loss (%)
15	0.080	0.21	24×10^{-6}	0.29	3.75	7.7
45	0.027	0.124	2.2×10^{-4}	0.15	12.5	1.2
135	0.0089	0.072	0.002	0.163	40	0.4

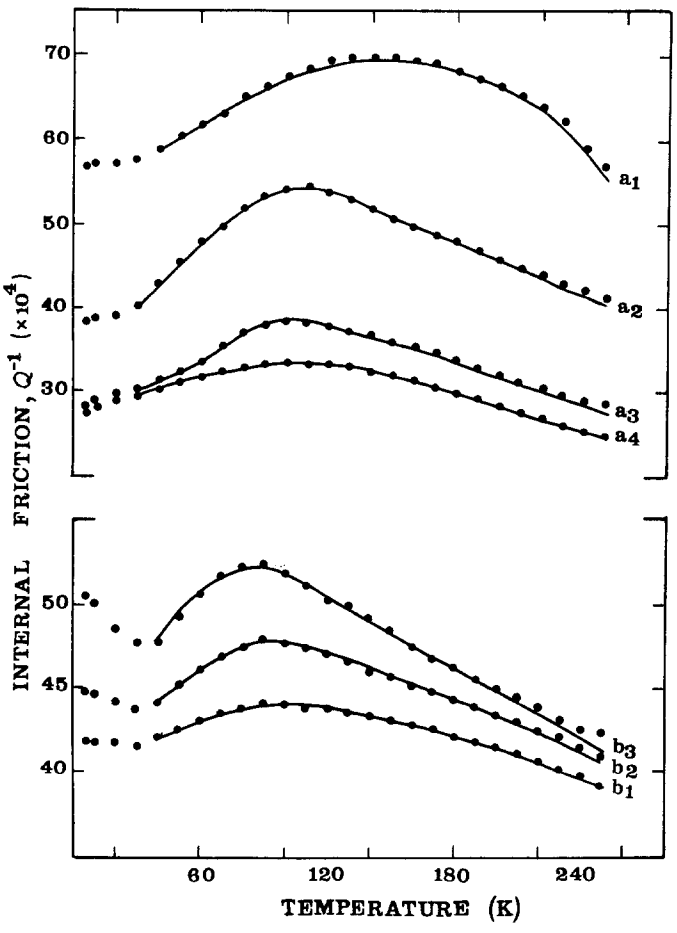

Figure 4 Internal friction of $CoO–P_2O_5$ glasses in the temperature range 6 to 300 K. Mole percentages of (CoO + Co_2O_3) are a_1 7.6, a_2 20.0, a_3 35.0, a_4 42.4, b_1 47.0, b_2 49.4, b_3 54.3.

fit of the TIC model at each measurement frequency (i.e. the relaxation spectrum of Fig. 6 substituted into Equation 23). In Fig. 9 the same exercise is performed for the TDC model by substitution of the data of Fig. 7 into Equation 28.

The scheme for computing the relaxation spectra was as follows, using 22 values of V_i with equal intervals ΔV between them. The chosen maximum and minimum values were about 0.22 and 0.03 eV, but varied slightly for each specimen, as also did ΔV in all cases as stated in Figs 6 and 7. Further, 22 different temperatures were selected in 10 K intervals, starting from 40 K, and 22 different corresponding values of Q^{-1} were read off the experimental 45 MHz loss curves. Substitution of all these Q^{-1}, V and T values into either Equation 23 or 28, and solving the resulting 22 simultaneous equations with 22 undetermined constants C_1, C_2, . . . , C_{22}, the spectrum of relaxation strengths for each glass can be obtained. The solution was effected by the use of the Gauss elimination method in a purpose-written Multics program run on the Honeywell mainframe computer of Brunel University.

Generally an exact solution thus obtained will contain some negative values of C_i, especially at high values of $V + \Delta V$, which can have no physical meaning. When this occurred the chosen values of V and ΔV were adjusted slightly until a solution involving only all positive C_i values was obtained. A smooth graph was then drawn through these values to ensure that these vlaues of C_i would reproduce the experimental Q^{-1} values which were much lower than the experimental values. So it proved necessary to increase the values of C_i at higher values of V in order to obtain better agreement with the experimental values. The upper and lower cut-off energies of 0.03 and 0.22 eV (see Figs 6 and 7) used in the above analysis have no physical significance but merely relate to the problems of computing.

The TDC spectra (Fig. 7) display a Gaussian form centred on a peak which corresponds closely to the "average" activation energy V_p determined in the usual manner from the frequency dependence of the peak temperature using Equation 12. At high values of V (see Fig. 7) C_i shows an increase with increasing V. These high values of C_i are required to give back the correct values of α (i.e. reproduce the experimental Q^{-1} at these high values of V). It is tempting to suggest that C_i should really fall off gradually with increasing V up to the end of our upper limit (which seems more physically plausible), or alternatively that we should truncate our C_i against V spectrum when it starts to increase at high V, for the purposes of regenerating Q^{-1} values. However, if this is done, one finds that Q^{-1} falls off very rapidly at high temperature rather than gradually, which is physically wrong. We do not know the reason for this behaviour. However, the situation could be ameliorated if a computer with a better capacity (i.e. $e^{\pm 150}$ rather than $e^{\pm 39}$) had been available, for then we would have found that the energy at which C_i started to rise again with V_i would be much higher. Then we could "truncate" the spectrum at a higher V value and we would have managed to reconstruct our experimental Q^{-1}–T curve over all the temperature range of interest, from a "sensible" shape for the C_i against V curves. In our subsequent calculations we have assumed that little error will result from assuming that the $\int C(V)\,dV$ for our

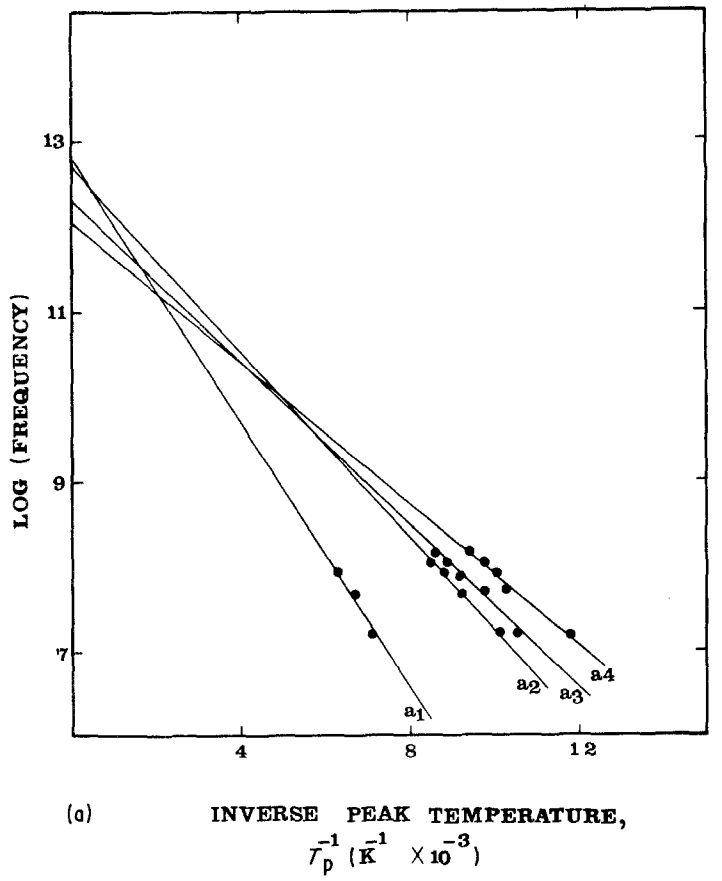

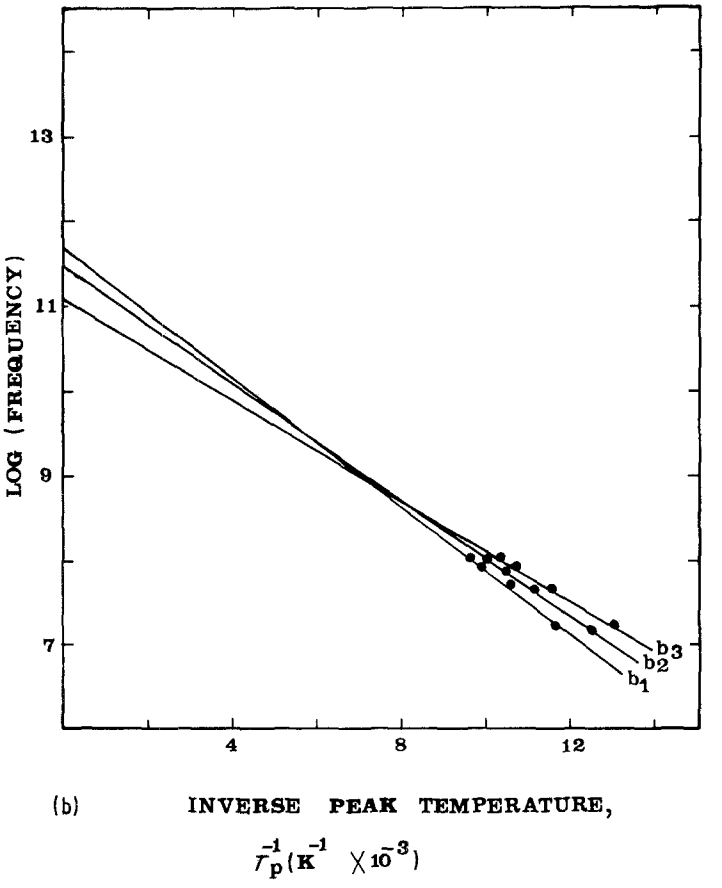

Figure 5 Plot of the relation $\omega(\tau_0)_p \exp(V_p/kT_p) = 1$, where T_p is the loss peak temperature and V_p is a constant for a given glass. Mole percentages of (CoO + Co_2O_3): (a) a_1 7.6, a_2 20.0, a_3 35.0, a_4 42.4; (b) b_1 47.0, b_2 49.4, b_3 54.3.

computed $C(V)$ spectrum (including the portion where $C(V)$ rises with V at high V) is the same as the area that would have been obtained using a better computer and the measures already described above.

5. Discussion

Over the temperature and frequency range considered the solid curves of the theoretical TIC plots match the experimental data very well – mostly within the reproducibility of the latter. In the case of the TDC plots the agreement is fair but generally the theoretical attenuation falls systematically below the experimental value, by an amount which increases with frequency. For example, at 135 MHz the shortfall is about −15%,

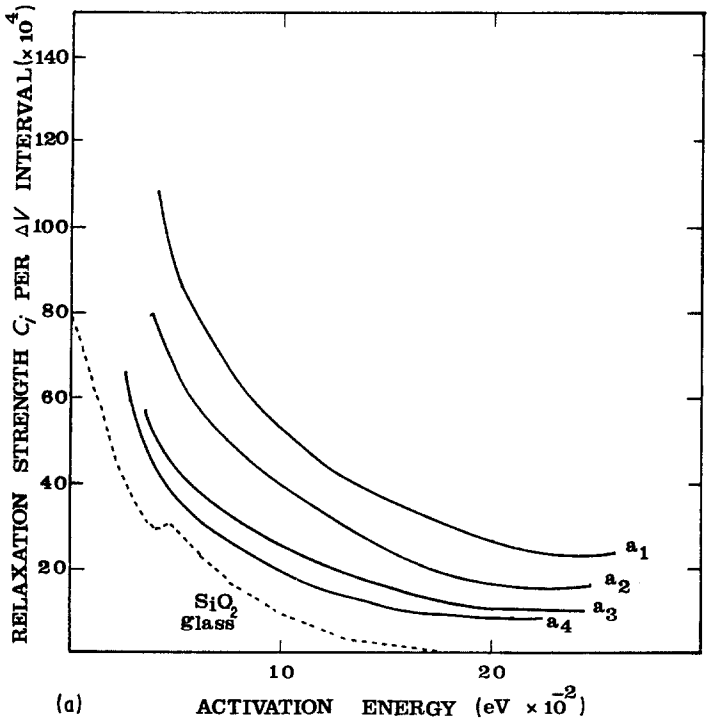

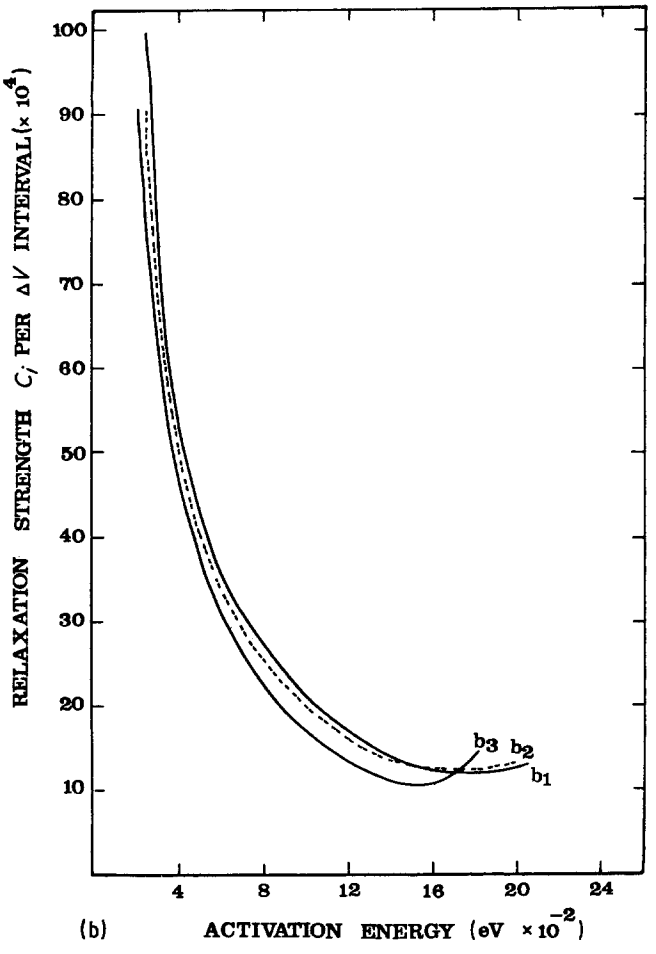

Figure 6 Relaxation spectrum obtained from a computer fit of the equation $Q^{-1} = \Sigma_i c_i \omega\tau_0 \exp(V_i/kT)/[1 + \omega^2\tau_0^2 \exp(2V_i/kT)]$ (Equation 23) to the observed internal friction Q^{-1} of compressional waves in CoO–P_2O_5 glasses (Table II) in the temperature range 40 to 240 K, and frequency range 15 to 135 MHz. The spectrum is appropriate to the TIC case (broad distribution of asymmetries). (a) Glasses a_1, a_2, a_3 and a_4 for which the summation intervals $(V_i - V_{i-1})$ are 0.0101, 0.0104, 0.0099, and 0.0092 eV, respectively. (b) Glasses b_1, b_2 and b_3 for which the summation intervals are 0.0083, 0.0087, and 0.0075 eV, respectively. Values of τ_0 are taken from Table II.

whilst the absolute error in the experimental value caused by not adopting the corrections described in Section 3, is only 0.4%. We have ignored residual attenuation losses in the relaxation spectra analysis. However, such losses due to phonon–phonon scattering and thermoelastic interactions will be several orders of magnitude less than the observed losses.

The above considerations suggest that on the two-well formalism a broad spread of asymmetries exceeding $\pm 2kT$ for $T = 240$ K is present in the glasses. The fractional difference between the relaxed and unrelaxed moduli of the glasses ($\int C(V)\mathrm{d}V = \Sigma C_i$ in the TDC model) varies systematically with glass composition (Table II and Fig. 10) and decreases linearly from about 0.1% for almost pure P_2O_5 glasses to a minimum of $\approx 0.04\%$ for a glass approximating to

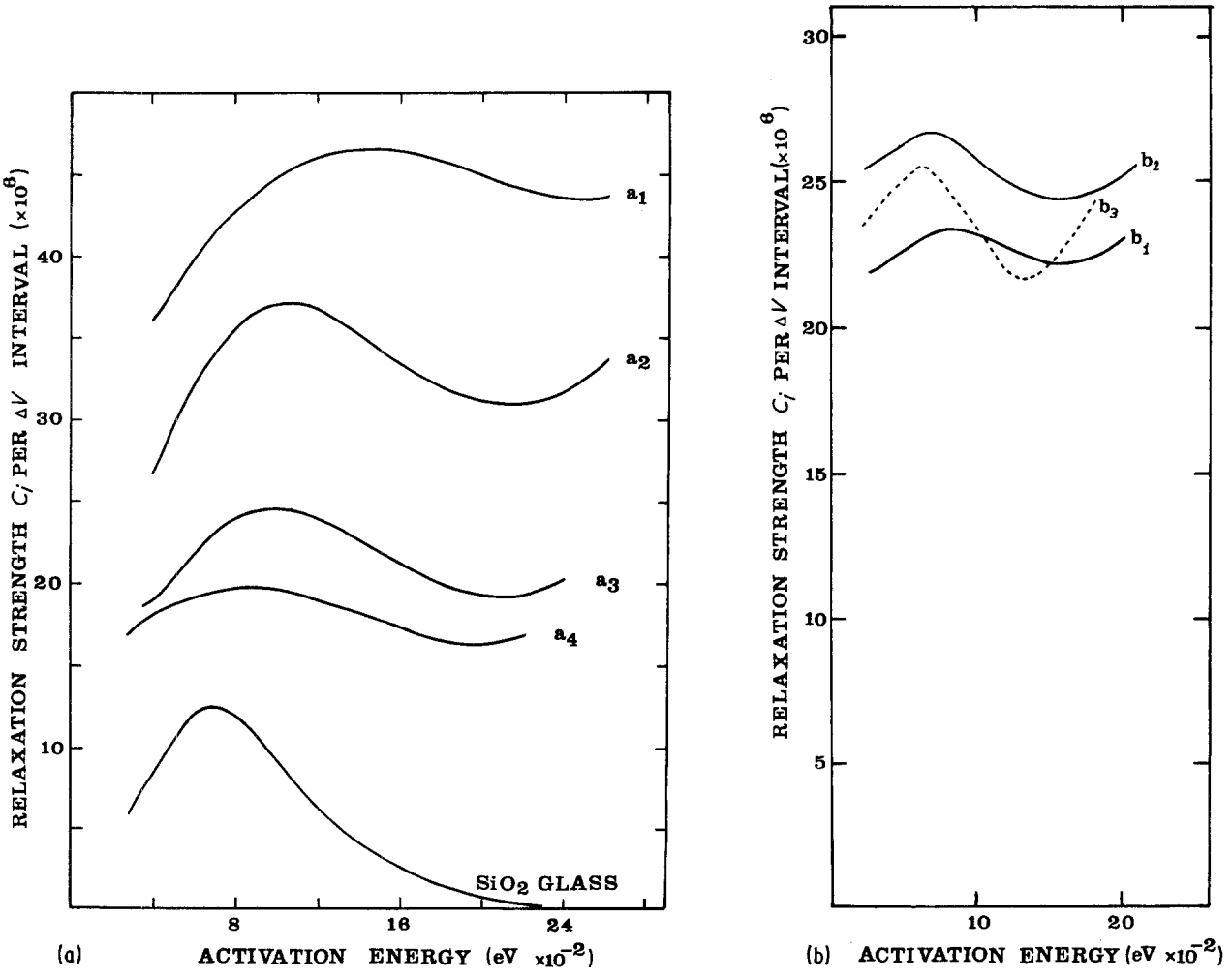

Figure 7 Relaxation spectrum obtained from a computer fit of the equation $Q^{-1} = (1/kT)\Sigma_i\, c_i\omega\tau_0 \exp(V_i/kT)/[1 + \omega^2\tau_0^2 \exp(2V_i/kT)]$ to the observed internal friction Q^{-1} of compressional waves in CoO–P_2O_5 glasses in the temperature range 40 to 240 K and frequency range 15 to 135 MHz. The spectrum is appropriate to the TDC case (narrow distribution of asymmetries). (a) Glasses a_1, a_2, a_3 and a_4 for which summation intervals ($V_i - V_{i-1}$) are 0.0101, 0.00104, 0.0099, and 0.010 eV, respectively, and for comparison the spectrum for vitreous SiO_2 with $V_i - V_{i-1} = 0.010$ eV. (b) Glasses b_1, b_2 and b_3 for which the summation intervals are 0.0083, 0.0087 and 0.0075 eV, respectively.

metaphosphate composition, $CoO(PO_3)_2$. Thereafter subsequent increase in CoO content produces a relatively small increase.

A similar striking composition dependence is seen in the shape of the TIC relaxation spectra. The value of V_i for which C_1 falls to e^{-1} of its peak value decreases from 0.135 for the almost pure P_2O_5 glass to 0.055 eV for the metaphosphate composition, thereafter remaining almost constant. A similar behaviour can be discerned in the half-widths of the peaks in the TDC relaxation spectra.

We suggest that the composition dependence of the above properties is evidence of the acoustic relaxation phenomena being a property of the glass network as a whole, i.e. it is to be associated with the various possible structural groupings of phosphorus with oxygen. Since rather similar composition dependences have been obtained with the MoO_3–P_2O_5 system it is difficult to reach any contrary conclusion [5–8].

Perhaps the most interesting information contained in the theoretical TIC plots is to be obtained from an examination of the experimental data in the low-temperature limit. If the solid lines in Fig. 8 are extrapolated below 40 K it is quite clear that they will

TABLE II Summary of low-temperature properties of cobalt–phosphate glasses

Glass No.	Density ($g\,cm^{-3}$)	Compressional wave velocity ($m\,sec^{-1}$)*	CoO + Co_2O_3 (mol %)	Peak temp. (K)	Peak loss (dB μsec^{-1})	Frequency, ν (MHz)	Attempt frequency, $(\tau_0)_p^{-1}$ ($\times 10^{13}$ Hz)	Average activation energy, V_p (eV)	$\int C(V)\,dV$ using TIC model ($\times 10^{-3}$)	$\int C(V)\,dV$ using TDC model ($\times 10^{-4}$)
a_1	2.685	4780	7.6	150	8.54	45.0	0.66	0.156	98.8	9.79
a_2	2.845	4861	20.0	109	6.66	45.0	0.47	0.114	67.6	7.49
a_3	2.892	4839	35.0	102	4.98	47.5	0.19	0.095	44.1	4.56
a_4	2.914	4845	42.4	98	4.39	47.5	0.12	0.084	38.0	3.55
b_1	2.985	4865	47.0	95	5.50	46.0	0.05	0.076	42.7	3.98
b_2	3.013	4894	49.4	90	5.86	45.0	0.03	0.068	47.1	4.72
b_3	3.133	5015	54.3	87	6.38	44.7	0.01	0.060	41.0	3.95

*Measured at room temperature. However, since the dispersion is small, it can be assumed equal to the quantity C in the text, when necessary.

fall increasingly below the data. We suggest that the departure is evidence of the existence of two-level systems, i.e. the relaxation of particles between split ground states starts to make a significant contribution to the acoustic loss in all the glasses at temperatures below 40 K. Indeed, in the two glasses containing the most CoO a second loss peak is observable at 105 MHz, at about 25 K. This is remarkably high since all previous reports [1, 2] on two-level relaxation peaks in other (non-phosphate) glass systems suggest that these peaks arise typically at temperatures of between 1 and 6 K.

6. Conclusions

(i) Acoustic relaxation phenomena in the CoO–P_2O_5 glass system in the frequency range 14 to 135 MHz and temperature range 6 to 300 K are consistent with the existence of an ensemble of two-well

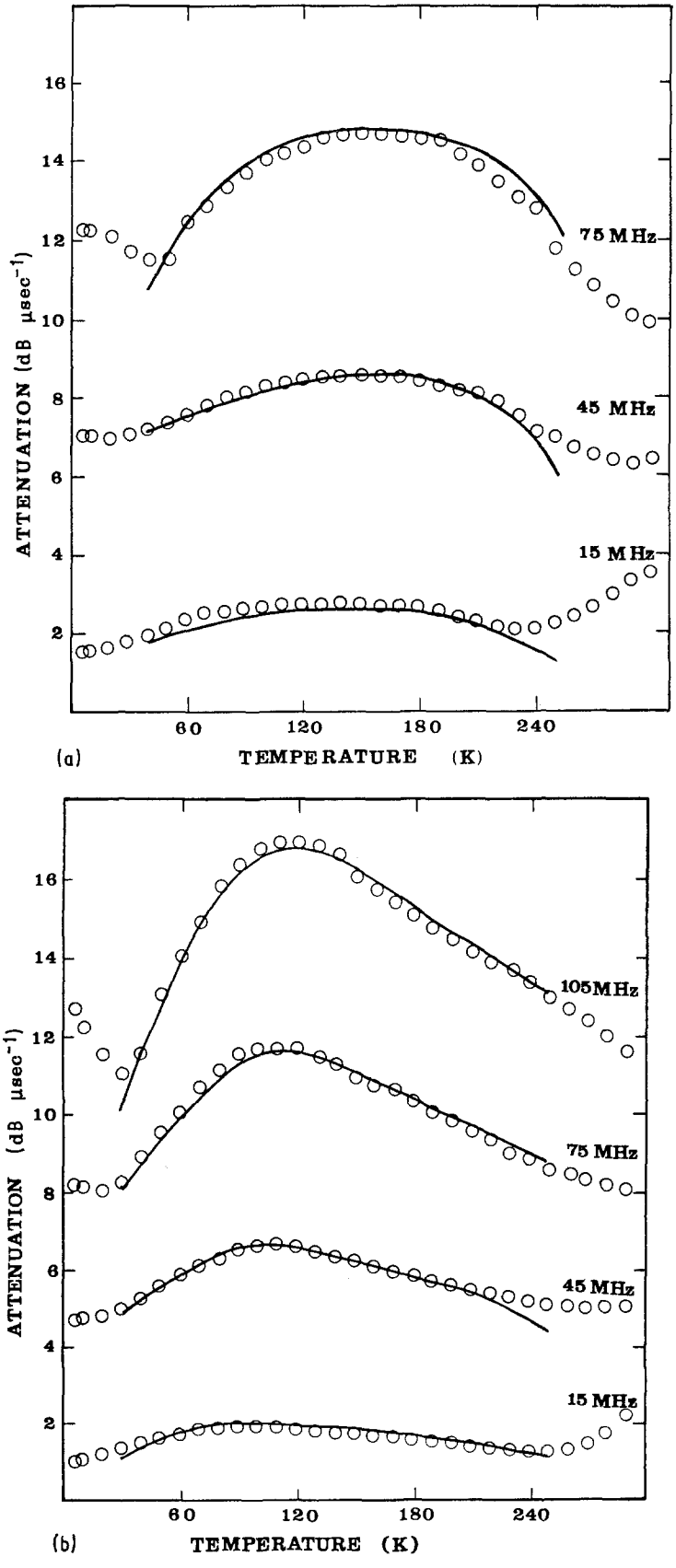

Figure 8 Temperature, frequency and composition dependence of ultrasonic compressional wave absorption in CoO–P_2O_5 glasses, below room temperatures. Hollow circles represent experimental data points and solid lines represent a theoretical fit of the equation $Q^{-1} = \Sigma_i c_i \omega\tau_0 \exp(V_i/kT)/[1 + \omega^2\tau_0^2 \exp(2V_i/kT)]$ (Equation 23, TIC case) using the relaxation spectra (C_i against V_i values) plotted in Fig. 6 (conversion of attenuation into units of dB μsec^{-1} using the relation $Q^{-1} = 2\alpha c/\omega$). (a) a_1, (b) a_2, (c) a_3, (d) a_4, (e) b_1, (f) b_2, (g) b_3.

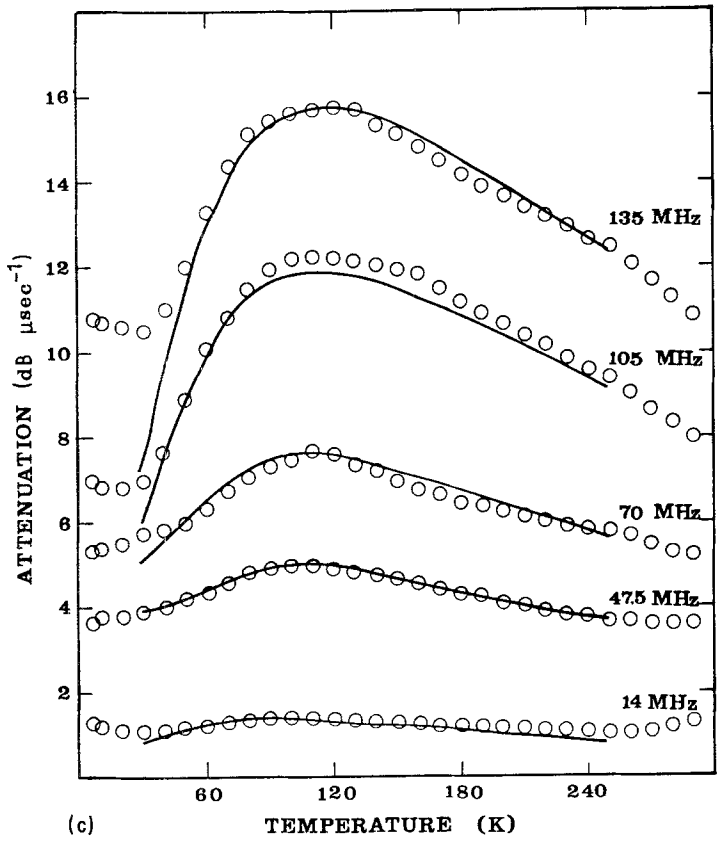

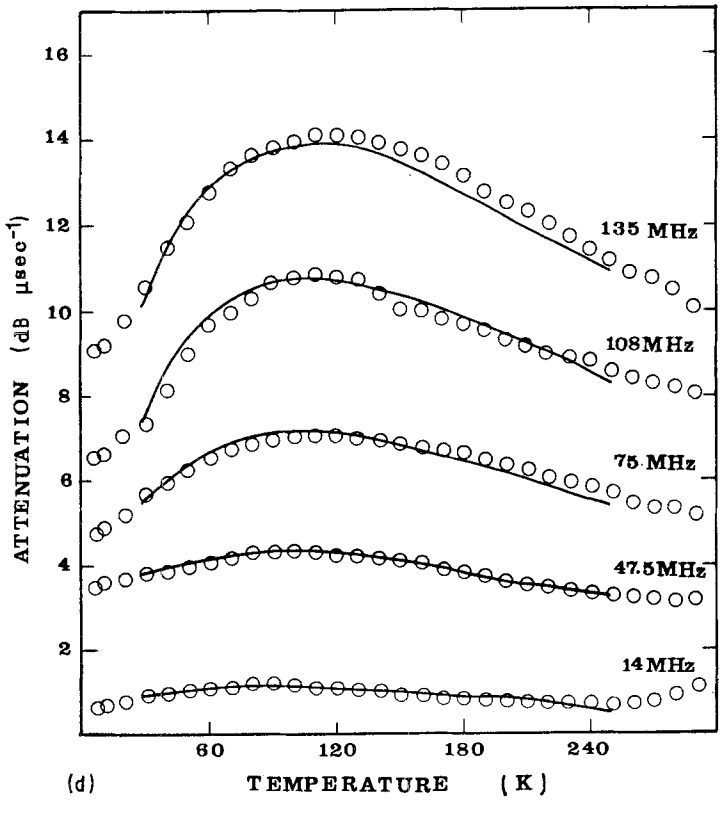

Figure 8 Continued.

systems of atomic dimensions with a range of barrier heights up to ≈ 0.2 eV and asymmetries up to ≈ 0.2 eV.

(ii) The relaxation spectrum of such an ensemble has been determined and found to vary systematically with composition. We suggest that a rather broad spectrum is to be associated with a network of P_2O_5 groupings, whilst a spectrum of less than one-half the width of the former is to be associated with metaphosphate groupings.

(iii) Confirmation that such a two-well model is more appropriate than one involving a narrow range of asymmetries requires an investigation to be carried out at higher frequencies. However, the level of peak loss obtaining in the glasses would render this difficult. Glasses would have to be made much thinner, and to avoid the problem of overlapping echoes when pulses are maintained long enough to yield a narrow frequency spectrum, it is probable that continuous-wave or buffer-rod techniques would be required.

(iv) Arguably one of the most useful applications of

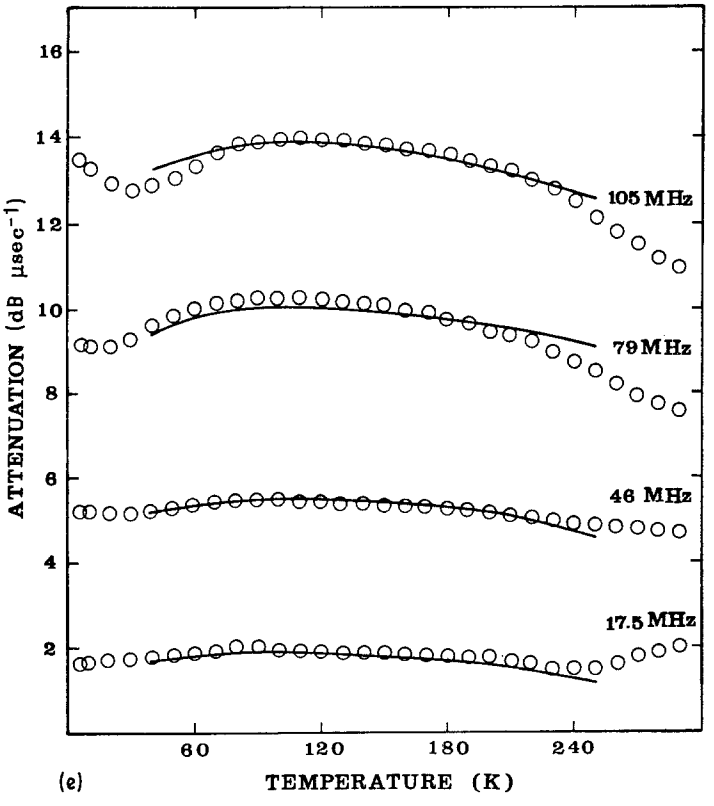

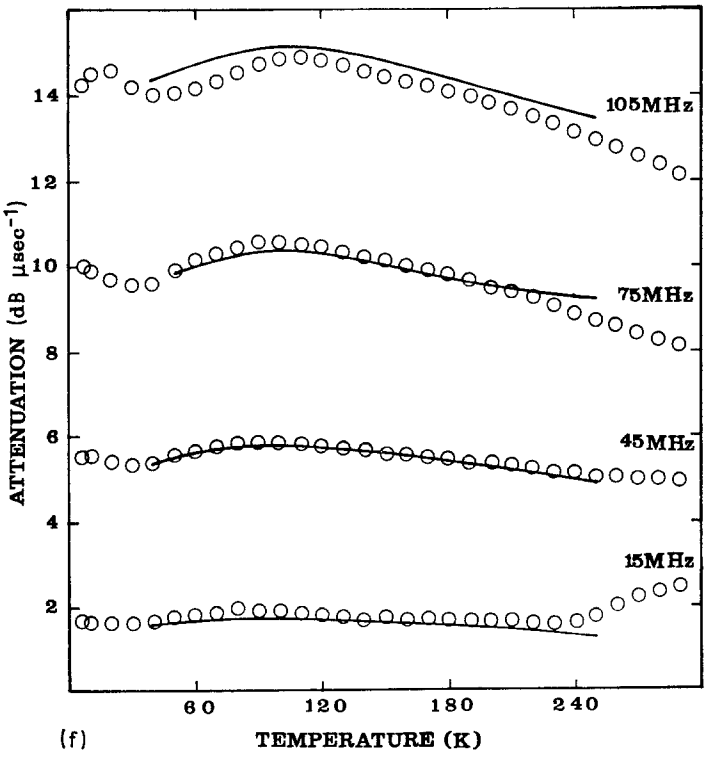

Figure 8 Continued.

a relaxation spectrum analysis is that the fractional difference between the relaxed and unrelaxed moduli can be evaluated from attenuation data alone. This result can then be compared with measurements of the frequency and tempeature dependence of phase velocity, to thus identify contributions to the dependence of velocity on these parameters caused by mechanisms other than two-well relaxation, for example lattice anharmonicity.

(v) The physical significance of relaxation spectra is questioned from time to time in the literature. Even so, one value of such analysis is that it provides an objective method if extrapolating experimental data. In this way the analysis has revealed evidence of the existence of two-level systems which produce a discernible relaxation loss at temperatures below 40 K.

Appendix

The following presentation is given because it is more straightforward than equivalent ones given in existing literature [13]. Unles stated otherwise the notation is as in the main text

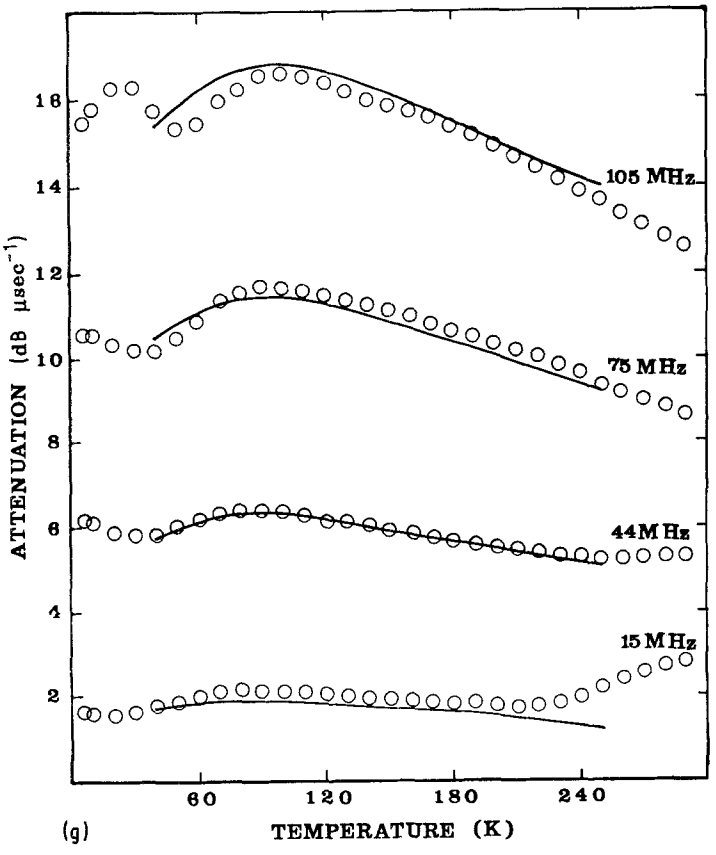

Figure 8 Continued.

A.1. Fractional difference between the relaxed and unrelaxed modulus caused by two-well systems

Consider a distribution of n identical two-well systems per unit volume, the potential energy minimum of the first well exceeding the minimum of the second well by an amount Λ in the absence of an applied strain. The equilibrium population of the first well will be $n[1 + \exp(\Lambda/kT)]^{-1}$, and this will also be the unrelaxed population in the presence of an acoustic strain. However, the relaxed population when a small applied strain $d\varepsilon$ charges Λ by an amount $d\Lambda$ will be $n[1 + \exp(\Lambda/kT)]^{-1}$. Each particle relaxing to the second well looses energy of amount $d\Lambda$, so that the

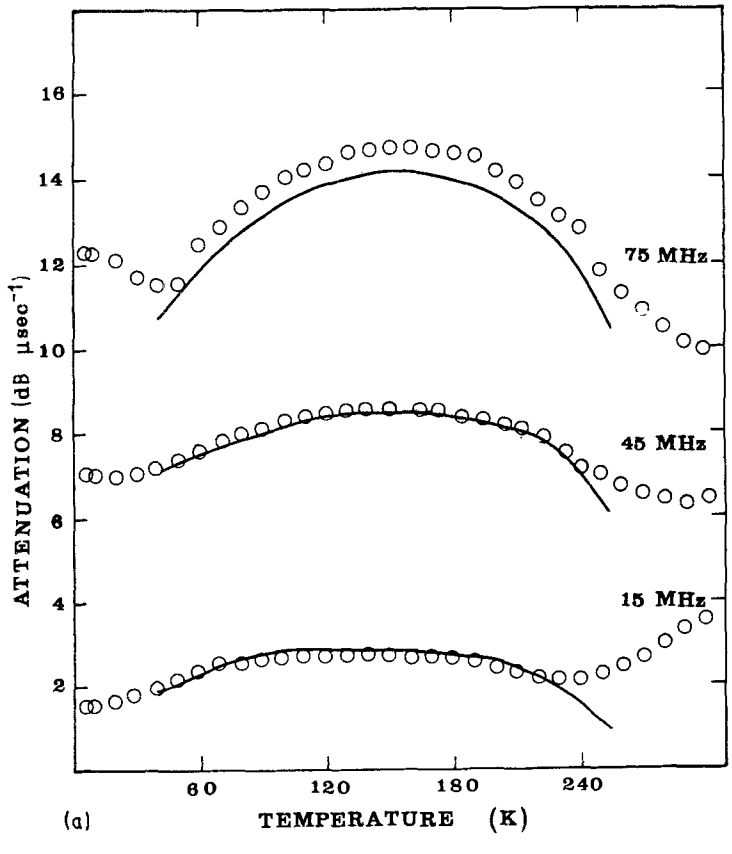

Figure 9 Experimental data of Fig. 8 but the solid lines represent a different theoretical fit, using the equation $Q^{-1} = (1/kT)\Sigma_i c_i \omega\tau_0 \exp(V_i/kT)/[1 + \omega^2\tau_0^2 \exp(2V_i/kT)]$ (Equation 28, TDC case) with the relaxation spectra (C_i against V_i values) plotted in Fig. 7 (conversion of attenuation into units of dB μsec^{-1} using the relation $Q^{-1} = 2\alpha c/\omega$, with α in nepers per unit length). (a) a_1, (b) a_2, (c) a_3, (d) a_4, (e) b_1, (f) b_1, (g) b_3.

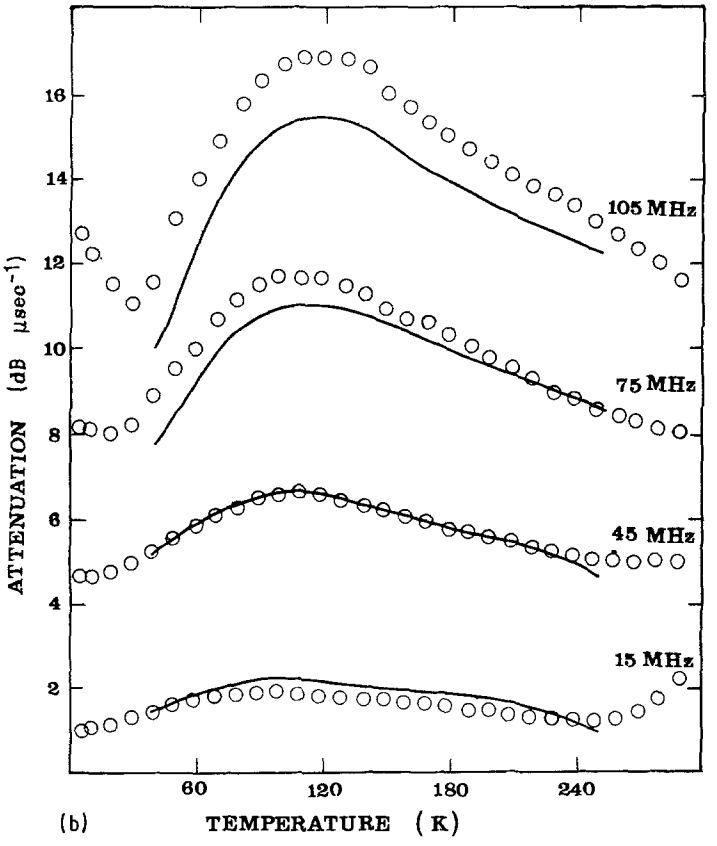

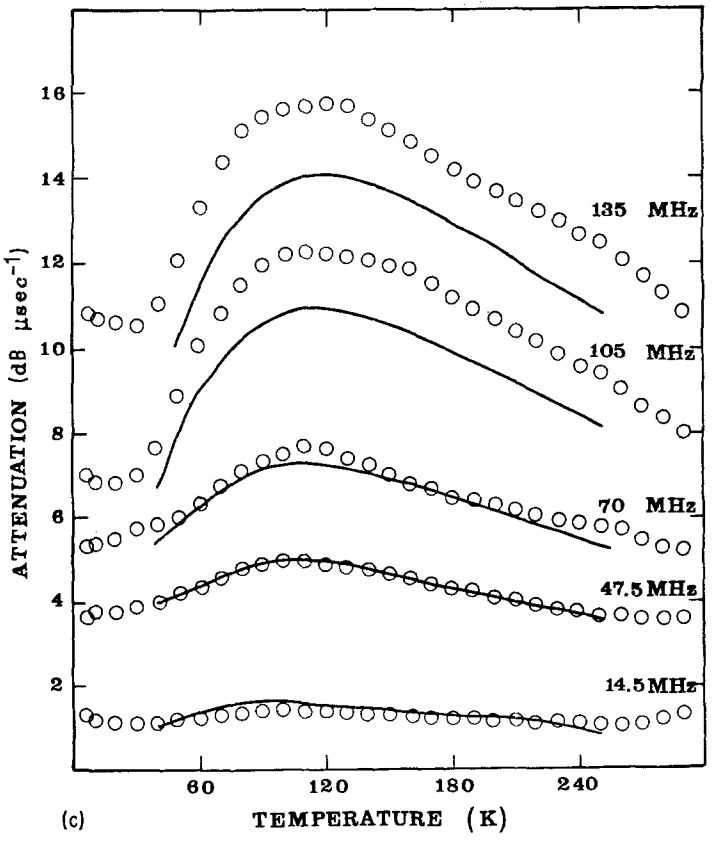

Figure 9 Continued.

difference between the stored energy per unit volume in the relaxed and unrelaxed states will be

$$\Delta U = -n\mathrm{d}\Lambda^2\left(\frac{\mathrm{d}}{\mathrm{d}\Lambda}\right)\left(\frac{1}{1+\left(\frac{\Lambda}{kT}\right)}\right) \quad \text{(A1)}$$

Now the stored elastic energy per unit volume due to the applied strain $\mathrm{d}\varepsilon$ is $M(\mathrm{d}\varepsilon)^2$ and $(M - \Delta M)(\mathrm{d}\varepsilon)^2$ in the relaxed and unrelaxed states, respectively. So $\Delta U = \Delta M(\mathrm{d}\varepsilon)^2$, in which case Equation A1 gives

$$\Delta M = -n\left(\frac{\mathrm{d}\Lambda}{\mathrm{d}\varepsilon}\right)^2\left(\frac{\mathrm{d}}{\mathrm{d}\Lambda}\right)\left(\frac{1}{1+\exp\left(\frac{\Lambda}{kT}\right)}\right) \quad \text{(A2)}$$

Writing $D = (\partial\Lambda/\mathrm{d}\varepsilon)$ and $M = \varrho c^2$, Equation A2

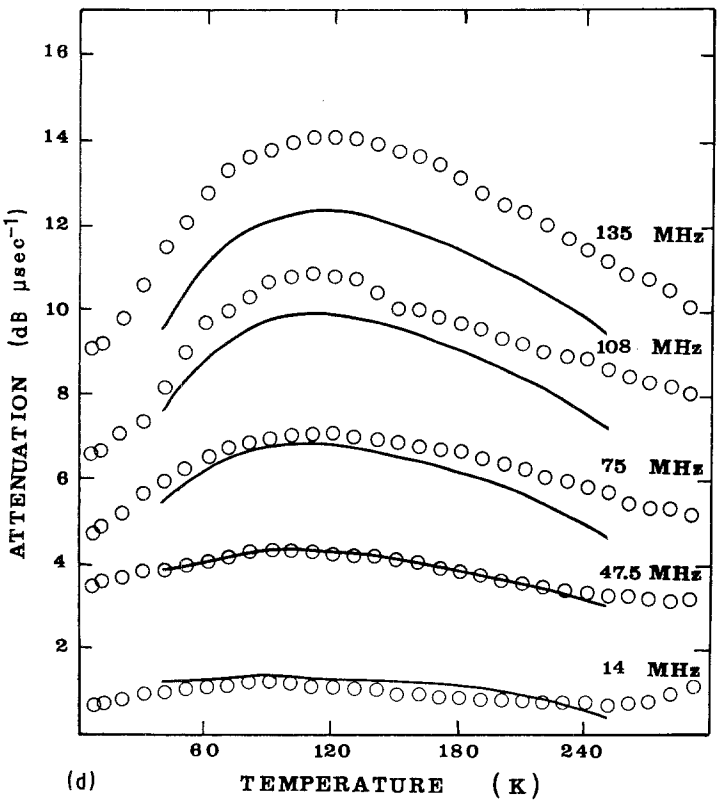

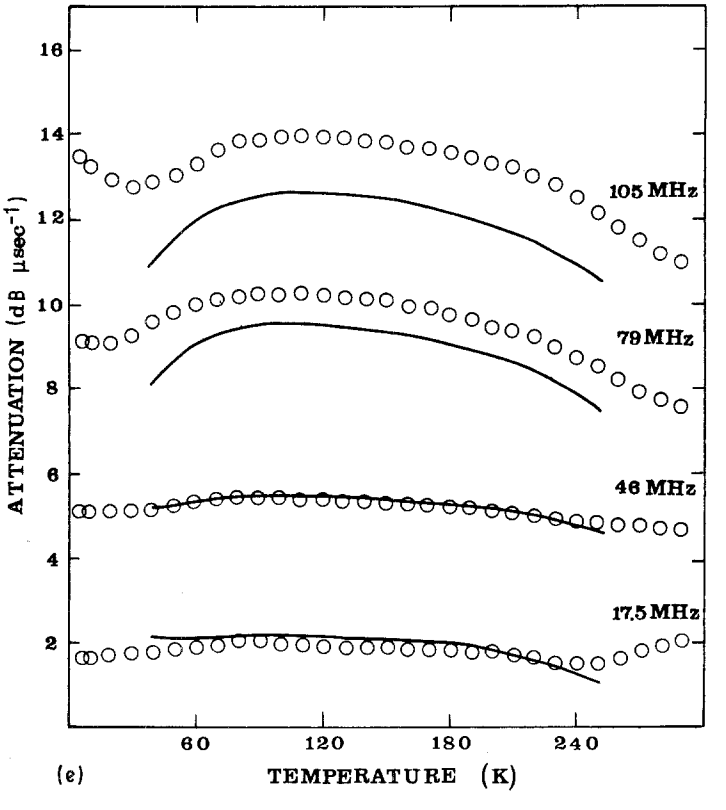

Figure 9 Continued.

becomes

$$\frac{\Delta M}{M} = -n\left(\frac{D^2}{\varrho c^2}\right)\left(\frac{\mathrm{d}}{\mathrm{d}\Lambda}\right)\left(\frac{1}{1 + \exp\left(\frac{\Lambda}{kT}\right)}\right) \quad \text{(A3)}$$

which is Equation 8 in Section 2.

A.2. Relaxation time

Let the barrier height measured from the bottom of the second well be V. The rate of change of the populations of the first wells, due to particle transitions from the first to the second wells and vice versa, are respectively

$$\left[\frac{\mathrm{d}n'}{\mathrm{d}t}\right]_{12} = \frac{-n'}{2\tau_0}\exp\left(\frac{-V}{kT}\right)\exp\left(\frac{\Lambda}{kT}\right)$$

and

$$\left[\frac{\mathrm{d}n'}{\mathrm{d}t}\right]_{21} = \frac{n - n'}{2\tau_0}\exp\left(\frac{-V}{kT}\right)$$

where n' is the instantaneous population of the first well and $1/2\tau_0$ is the classical vibration frequency of

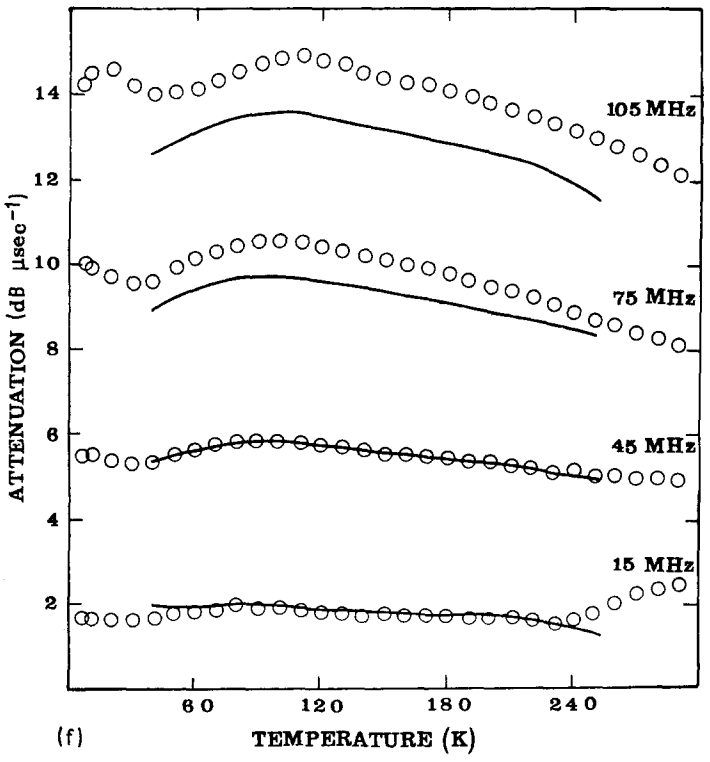

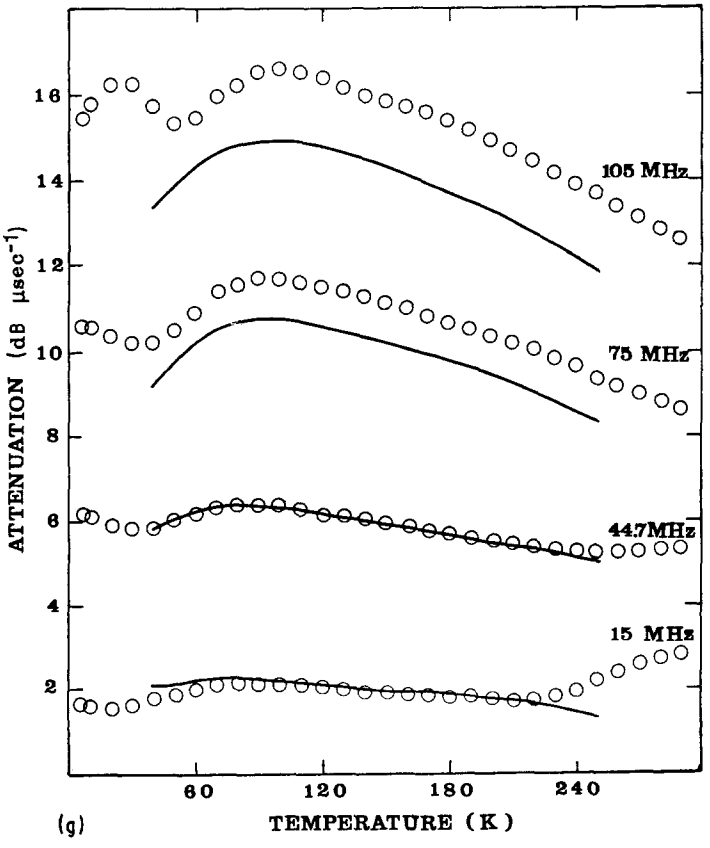

Figure 9 Continued.

the particles in either well, assuming that these frequencies are equal. As will subsequently become apparent, the factor of 2 is introduced to produce a convenient notation at the end-point of our calculation. The net rate of population change in the first wells is

$$\left[\frac{dn'}{dt}\right] = \left[\frac{dn'}{dt}\right]_{12} + \left[\frac{dn'}{dt}\right]_{21}$$

$$= \frac{-n'}{\tau_0}\exp\left(\frac{-V}{kT}\right)\left[1 + \exp\left(\frac{\Lambda}{kT}\right)\right] + \frac{n}{\tau_0}\exp\left(\frac{-V}{kT}\right)$$

so

$$\left[\frac{dn'}{dt}\right] + \frac{n'}{\tau} = q \qquad \text{(A4)}$$

where

$$\tau = 2\tau_0 \exp\left(\frac{V}{kT}\right)\left[1 + \exp\left(\frac{\Lambda}{kT}\right)\right]^{-1}$$

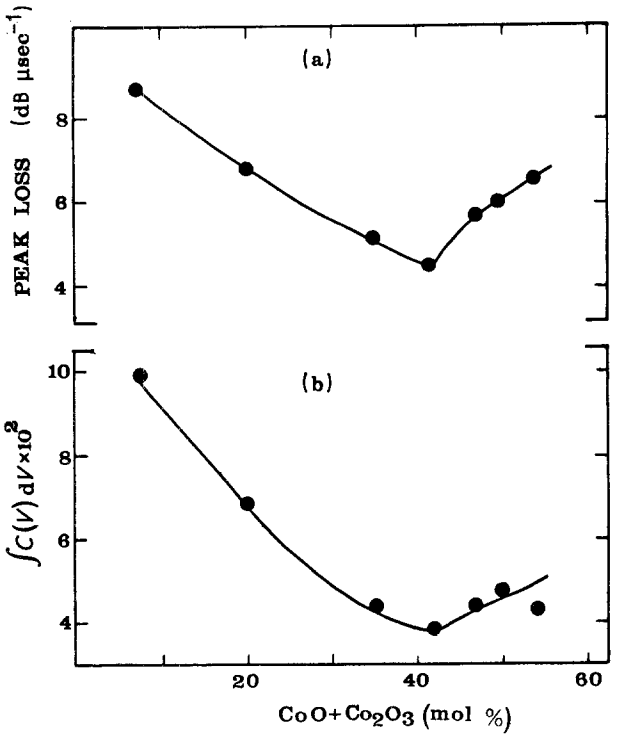

Figure 10 Composition dependence of (a) peak loss and (b) fractional difference between relaxed and unrelaxed elastic moduli ($\int C(V)\,dV$) of CoO–P_2O_5 glasses, arising from the TIC theory (Equation 23 and the relaxation spectrum of Fig. 6).

and

$$q = \frac{n}{\tau_0}\exp\left(\frac{-V}{kT}\right)$$

After an arbitrary initial disturbance, subsequently removed, solution of Equation A4 shows that n' decays to an equilibrium value of $q\tau = [1 + \exp(\Lambda/kT)]^{-1}$ at a rate $\exp(-t/\tau)$; thus Equation A3 can be associated with the relaxation time occurring in Equations 1 to 3 and 5 and 6 defining the properties of the standard linear solid.

If, alternatively, V is measured from the potential half-way between the two-well minima, it follows that

$$\tau = 2\tau_0 \exp\left(\frac{+V}{kT}\right)\exp\left(\frac{\Lambda}{2kT}\right)\left[1 + \exp\left(\frac{\Lambda}{kT}\right)\right]^{-1}$$

$$= \tau_0 \exp\left(\frac{V}{kT}\right)\operatorname{sech}\left(\frac{\Lambda}{2kT}\right) \quad \text{(A5)}$$

a notation favoured by some authors.

References

1. S. HUNKLINGER and W. ARNOLD, in "Physical Acoustics", Vol. 12, edited by W. P. Mason and R. N. Thurston (Academic, New York, 1976) p. 155.
2. S. HUNKLINGER and M. V. SCHICKFUS, in "Amorphous Solids, Low Temperature Properties", Vol. 6, edited by W. A. Phillips (Springer, Berlin, 1981) p. 81.
3. N. D. PATEL, PhD thesis, Brunel University (1982).
4. A. A. HIGAZY, PhD thesis, Brunel University (1984).
5. B. BRIDGE and N. D. PATEL, *J. Mater. Sci.* **21** (1986) 3783.
6. *Idem, J. Mater. Sci. Lett.* **5** (1986) 1198.
7. B. BRIDGE, *ibid.* **5** (1986) 1203.
8. B. BRIDGE and N. D. PATEL, *ibid.* **5** (1986) 1255.
9. *Idem. J. Mater. Sci.* (1987) 781.
10. K. S. GILROY and W. A. PHILLIPS, *Phil Mag.* **B43** (1981) 735.
11. S. HUNKLINGER, "Ultrasonics Symposium Proceedings" (IEEE, New York, 1974) p. 443.
12. A. K. JONSCHER, "Dielectric Relaxation in Solids", (Chelsea Dielectrics Press, London, 1983) Chs 7 and 8.
13. J. JÄCKLE, L. PICHE, W. ARNOLD and S. HUNKLINGER, *J. Non-Cryst. Solids* **20** (1976) 365.
14. A. A. HIGAZY and B. BRIDGE, *Phys. Chem. Glasses* **26**(3) (1985) 82.
15. *Idem, J. Non-Cryst. Solids* **72** (1985) 81.
16. R. TRUELL, C. ELBAUM and B. B. CHICK, "Ultrasonic Methods in Solid State Physics" (Academic, New York, 1969) pp. 89–135.
17. H. J. McSKIMIN, *J. Acoust. Soc. Amer.* **20** (1956) 484.

Received 5 February
and accepted 28 April 1987